

# Preparation and commissioning for the LHD deuterium experiment

Masaki Osakabe<sup>1,2</sup>, Mitsutakam Isobe<sup>1,2</sup>, Masahiro Tanaka<sup>1,2</sup>, Gen Motojima<sup>1,2</sup>, Katsuyoshi Tsumori<sup>1,2</sup>, Masayuki Yokoyama<sup>1,2</sup>, Tomohiro Morisaki<sup>1,2</sup>, Yasuhiko TAKEIRI<sup>1,2</sup> and LHD Experiment Group

<sup>1</sup>National Institute for Fusion Science, National Institutes of Natural Sciences, Toki 509-5292, Japan

<sup>2</sup>SOKENDAI(The Graduate University for Advanced Studies), Toki 509-5292, Japan

**Abstract**— The deuterium experiment started from March, 2017 on the Large Helical Device (LHD) as a part of LHD high-performance upgrade project. The objectives of the deuterium experiment is (1) to realize the high performance operation, (2) to explore the physics of isotope effect, (3) to demonstrate the confinement capability of energetic particles in helical devices, and (4) to explore the research on plasma material interactions using the benefit of stable steady state operation ability of LHD. As preparations for deuterium experiment, the positive-ion based Neutral Beam Injectors (NBIs) are upgraded to increase their injection power in deuterium operation. On the other hand, the injection power of negative-ion based NBI is deteriorated due to the isotope effect of negative-ion source. The neutron diagnostic and the exhaust detritiation system are newly installed for the deuterium experiment. The commissioning of LHD for the deuterium experiment is quite successful. The high ion temperature operation region is extended by the deuterium experiment. Ion temperature exceeding 9keV is achieved with the deuterium operation of LHD.

**Index Terms**—LHD, deuterium experiment, Heliotron, Stellarator, isotope effect, negative-ion source, neutron diagnostic, fuel mass balance, steady state operation

## I. INTRODUCTION

THE deuterium experiment has been conducted since March 2017 on the Large Helical Device (LHD) as a part of the LHD high-performance upgrade project [1], which includes the upgrade of heating devices, the installation of closed helical divertor [2], [3], [4] and the upgrade for diagnostic systems. The objectives of the deuterium experiment are [1],[5]:

- (1) to realize high-performance plasmas in helical systems by confinement improvement and by upgraded facilities;
- (2) to study the isotope effects on plasma confinement in

This paper was submitted on July 19, 2017. The LHD experiment and all of NIFS activities have been continuously and strongly supported by The Ministry of Education, Culture, Sports, Science and Technology (MEXT), Japan, and domestic and international collaborators.

M. Osakabe is with the National Institute for Fusion Science under the National Institutes of Natural Sciences, Toki, Gifu 509-5292 Japan. He also belongs to SOKENDAI (The Graduate University for Advanced Studies) with the same mailing address to NIFS. (e-mail: osakabe.masaki@LHD.nifs.ac.jp).

- toroidal plasma devices [6], [7], [8], [9], [10];
- (3) to demonstrate the confinement capability of Energetic Particles (EPs) in helical systems; and
  - (4) to extend the research on the Plasma-Material Interactions (PMI) with long time scale using the benefits of the LHD's steady state operation ability.

As shown in Table 1, nine years of the deuterium experiment campaign are planned and are divided into two periods. The first half period consists of 6 years of experiment campaign, where the annual yield of neutron and tritium are limited to  $2.1 \times 10^{19}$  neutrons and 37GBq, respectively. In this period, we will focus on the characterization of deuterium plasmas on LHD. In particular, the first year of the deuterium experiment is dedicated to the commissioning of deuterium experiment. The latter half period consists of 3 years of experiment campaign, where the annual yield of neutron and tritium are limited to  $3.2 \times 10^{19}$  neutrons and 55.5GBq, respectively. Based on the knowledge accumulated during the first half period, the exploration in the integrated high performance discharge scenarios will be conducted.

As a preparation for the deuterium experiments, the positive-ion based Neutral Beam Injector (NBI) was upgraded to increase its injection power by increasing its injection energy. The beam energy can be increased without the deterioration of neutralization efficiency of ion beam by changing the beam ion

TABLE I  
SCHEDULE OF DEUTERIUM EXPERIMENTS ON LHD

Fiscal Year	1st year (19th LHD experiment cycle)	2nd – 6th year	7th - 9th year
Experiment	Preliminary (commission- ing)	Exploration and characteriza- tion of deuterium plasmas	Integrated high- performance experiments
Maximum Annual Neutron Yield		$2.1 \times 10^{19}$ [n]	$3.2 \times 10^{19}$ [n]
Maximum Annual Tritium Yield		$3.7 \times 10^{10}$ [Bq]	$5.55 \times 10^{10}$ [Bq]

species from hydrogen to deuterium because the neutralization efficiency is a function of the beam particle velocity, i.e., the function of beam energy per nucleon. On the other hand, the injection energy of the negative-ion based NBI remains the same as the hydrogen operation in order to suppress the neutron emission from LHD plasmas. Thus, the decrease of its injection power is a concern due to the mass dependence of optimum beam extraction condition. The detail of the deuterium operation of NBI is discussed in section 2.

The neutron diagnostic is newly installed for the deuterium experiment on LHD. One of the most important roles for this diagnostic is the evaluation of total neutron yield from LHD. The evaluation is necessary because LHD is classified as a legal radiation emitting device with the start of the deuterium experiment. The evaluation of energetic particle confinement property is another important role of the neutron diagnostic. For the accurate evaluation of the total neutron yield from LHD plasmas, the calibration experiment using a  $^{252}\text{Cf}$  neutron source of 800MBq was performed on LHD. In section 3, the neutron diagnostic on LHD and its calibration are briefly described. Initial results of neutron emission from LHD deuterium plasmas are also shown in the section. The detailed explanation for the neutron diagnostic can be found in elsewhere [11].

As a preparation for the deuterium experiment, the Exhaust Detritiation System (EDS) was also installed on LHD under the agreement on the environmental conservation with local governmental bodies. All of the vacuum exhaust gases from LHD and its peripheral devices are accumulated in the EDS and

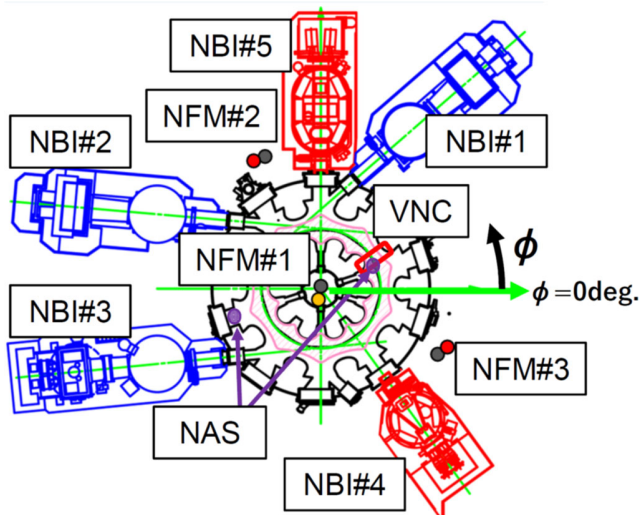


Fig.1 Schematic drawing of the LHD midplane. Three tangential NBI, based on negative-ion sources and named as NBI#1, NBI#2 and NBI#3, are installed on LHD. Two radial NBI, based on positive-ion sources and named as NBI#4 and NBI#5, are also installed. Location of three Neutron Flux Monitors (NFM) are also shown. The NFM#1 locates at the center of LHD and on the top of LHD. It consists of a  $^{235}\text{U}$  Fission chamber (●) and a  $^{10}\text{B}$  proportional counter (●). The NFM#2 and #3 locate outboard side of the LHD and at the height of the midplane. Each of them consists of a  $^{235}\text{U}$  fission chamber and a  $^3\text{He}$  proportional counter (●). The location of Vertical Neutron Camera (VNC) is shown by a rounded square and those of Neutron Activation foil System (NAS) are shown by purple circles (●). The direction of toroidal angle ( $\phi$ ) in Fig.4 is also shown in the figure.

all of the hydrogen isotopes as well as tritium are removed from the gas by converting them to water using catalyst. Because the tritium monitoring system is equipped with the inlet and the outlet of the EDS, the system can be utilized for the detailed analysis of mass balance studies for hydrogen isotopes on LHD using the tritium produced in the deuterium plasmas as a tracer. This will provide useful information for future fusion reactor in evaluating the fuel mass balance. The initial results of the measurement are shown in section 4.

The first deuterium experiment on LHD is started since March 7, 2017, on LHD as a part of the 19th LHD experiment cycle. The first four weeks of the 19th experiment cycle were dedicated for hydrogen experiments to prove that the operation of the LHD, its heating devices, its diagnostic systems, the EDS, and their interlock systems are proper to start the deuterium experiment. After the four weeks of hydrogen operation, the first deuterium experiment is started with deuterium operation of positive-ion NBIs in order to maximize the NB injection power and to suppress the neutron emission rate until the end of April, which correspond to the 8th week of the 19th cycle. This period is set to investigate the effect of radiations to the control system of LHD and its peripheral devices. The trial to extend the performance of LHD is also performed in this period. From the second week of May to the week of June 19-23, the negative-ion NBIs also start their deuterium operation and the neutron emission rate from LHD plasmas is maximized. This period is set to investigate the energetic-particle confinement property in LHD and the impact of isotope effects in LHD under the full deuterium operation of NBIs. The isotope effect on negative-ion sources of the LHD-NBI is also investigated in this period. The radiation effects on LHD and on the peripheral devices are also investigated with maximized neutron emission rate condition in this period. From the last week of June to the first week of July, the negative-ion based NBIs are operated in hydrogen again in order to set the second high power NBI heating period. The first deuterium experiment is terminated at the first week of July and the hydrogen experiment phase is restarted from the 2nd week of July for four weeks. The plasma experiments in the 19th cycle ends at August 3, 2017. This hydrogen experiment period is set to evaluate the necessary period for replacing the deuterium by hydrogen in the materials of the plasma counter wall. It is important to evaluate the necessary period for the replacement from hydrogen to deuterium and from deuterium to hydrogen after the change of working gas in plasmas. The variation of deuterium fraction in plasmas after the start of the deuterium experiment is shown in section 5 with the initial result of the deuterium experiment. Concluding remarks are provided in section 6.

## II. DEUTERIUM OPERATION OF LHD-NBI

Figure 1 shows the drawing of the LHD mid-plane and the location of peripheral devices. Three tangential Neutral Beam Injectors (tNBIs) and two radial NBIs (rNBIs) are installed on LHD. The tangential NBIs are named as NBI#1, NBI#2 and NBI#3. They are using negative-ion sources and their nominal injection power and energy are 5MW and 180keV, respectively,

when they operate with hydrogen beam [12], [13]. The radial NBIs are named as NBI#4 and NBI#5. They consist of 4 positive-ion sources, respectively. Their nominal injection power and energy are 6MW and 40keV, respectively, when they operate with hydrogen beam.

For deuterium operation, the rNBIs were upgraded to increase their injection power from 6MW to 9MW by increasing their injection energy from 40keV to 60keV for NBI#4 and to 80keV for NBI#5. This upgrade is possible because the neutralization efficiency does not deteriorate when the beam energy is doubled with the change of beam ion species from hydrogen to deuterium. The neutralization efficiency of hydrogen isotope ion beam is determined by the beam velocity, i.e., the particle energy normalized by its mass, because the cross sections of related atomic processes are the function of particle velocity. Figure 2(a) and (b) show the comparison of the arc-efficiencies between the hydrogen and the deuterium operation and that of power fractions of each energy components of NB from a ion-source of NBI#5. For positive-ion based NBI, three energy components of NBs are

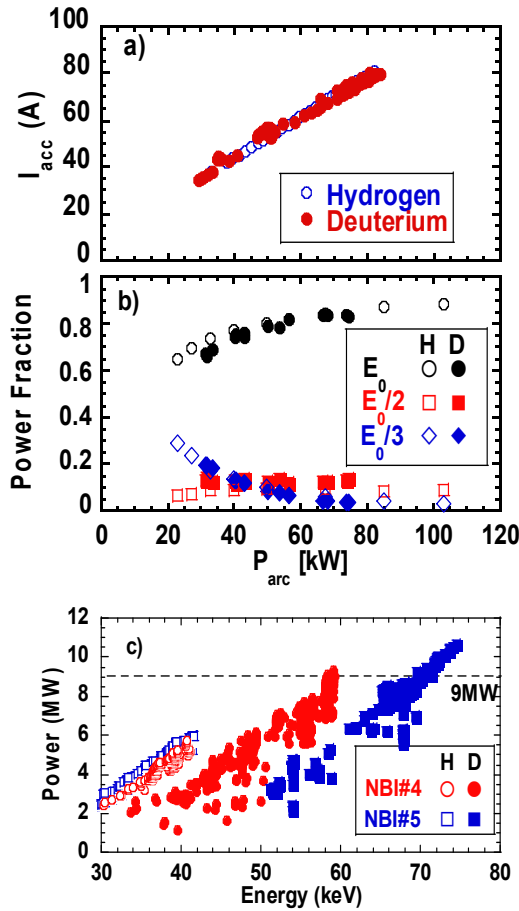


Fig. 2 (a) Arc power dependence of a positive-ion source used for NBI#5 are shown for hydrogen (○) and deuterium (●) and (b) arc power dependence of power fraction of Full (circles)-, 1/2 (squares)- and 1/3 (diamonds)- energy component of neutral beam from the source were shown for hydrogen (open symbols) and for deuterium (closed symbols). (c) Achieved injection NB power against beam energy are shown for NBI#4 (circles) and NBI#5 (squares) with hydrogen operation (open symbols) and those with deuterium operation (closed symbols).

produced because three types of positive ions, e.g.,  $H^+$ ,  $H_2^+$  and  $H_3^+$  for hydrogen operation, are produced for hydrogen isotopes. As shown in the figures, no significant differences are observed between hydrogen and deuterium operation for positive-ion sources. The achieved powers of positive-ion NBIs are shown in Fig.2(c). With the proper optimization of the ion source configuration, i.e., the proper optimization of gap distances between electrodes for acceleration, the operation of 9MW injection power were achieved both for NBI#4 and NBI#5 in deuterium beam operation.

The tNBI consists of two large negative-ion sources [12]. To suppress the neutron emission by the reaction between beam and thermal ions in LHD plasmas, it was decided to keep the beam energy at 180keV for the deuterium operation following upon the hydrogen operation. Because the isotope effect is recognized in negative-ion production process, i.e., the fraction of co-extracted electron to negative-ion beam is higher in deuterium than in hydrogen [14], [15], and because the mechanism of the isotope effect in negative-ion production is not fully understood yet, we have decided to use the negative-ion sources as they are, i.e., keeping the same ion source configuration to the hydrogen operation. Thus, it was expected that the beam power of the tangential-NBI would degrade to the 0.7 of the injection power in the hydrogen operation because the optimum beam condition is dominated by the Child-Langmuir law [16] where the optimum beam current density is scaled as the inverse square root of the mass of beam species. Figure 3 shows the variation of injection power of NBI#3 and the fraction of electron current to negative-ion current of negative-ion sources for NBI#3 before and after the change of operation gas from hydrogen to deuterium. As shown in Fig.3(a), the beam injection power of

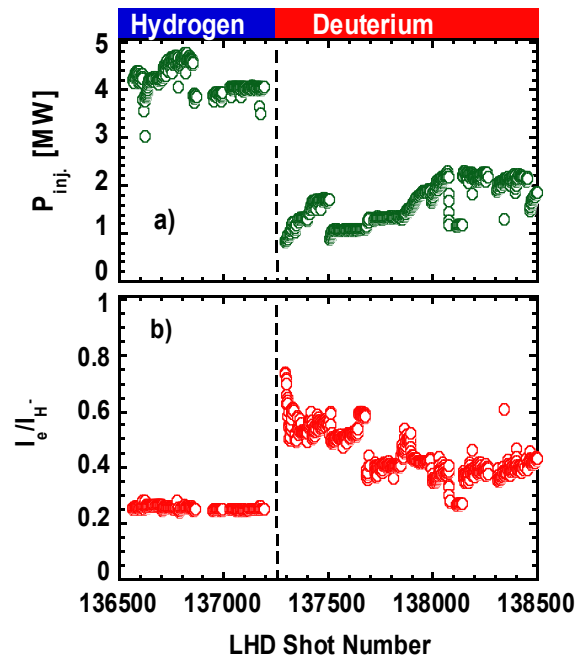


Fig. 3 Variation of (a) injection power and (b) the ratio of co-extracted electron current to the negative-ion current.

NBI#3 was reduced to one-half of the hydrogen operation after the change of operation gas to deuterium. After the change of the gas from hydrogen to deuterium, the fractions of co-extracted electron current to negative-ion current are increased from 0.2 to 0.4. This increases the heat load onto the electrodes of ion sources by co-extracted electrons and limits the allowable beam current extracted from the ion sources. Thus, the beam injection power of tangential-NBI is limited to around 2MW to suppress the heat load onto the electrodes by the co-extracted electrons with the deuterium negative-ion beam operation.

The decrease in injection power of tNBI causes another problem. On LHD, the plasma initiation by NBI is possible when the tangential-NBI is operated with hydrogen [17], [18], [19]. But, it becomes almost impossible to initiate the plasma by NBI when the tNBI is operated with deuterium. This is partly because the injection power of tNBI is decreased with deuterium operation. In addition, the normalized beam energy by its mass was decreased with the increase of the mass. This increases the charge exchange loss of energetic ions produced by the tNBI because the charge exchange cross section drastically changes at the energy range above 100keV/amu [20]. The increase of the charge exchange loss is crucial for plasma initiation by NBI because the small charge exchange cross section of energetic ions produced by the hydrogen tNBI plays an important role for the plasma initiation by NBI on LHD [17].

### III. EVALUATION OF NEUTRON EMISSION FROM LHD

The neutron diagnostic is the one of the most important diagnostics prepared for the deuterium experiment on LHD because the monitoring of total neutron yield, which is necessary for radiation safety control as a legal radiation emission device, is done according to the measurement by this diagnostic. Moreover, the neutron diagnostic is a powerful tool to evaluate the energetic particle confinement property during the deuterium experiment because the most of neutrons produced from the deuterium plasmas are the reaction between thermal ion and beam ion produced by the NBI on LHD [1].

On LHD, three sets of Neutron Flux Monitors (NFM) are installed for this purpose as shown in Fig.1. Each NFM

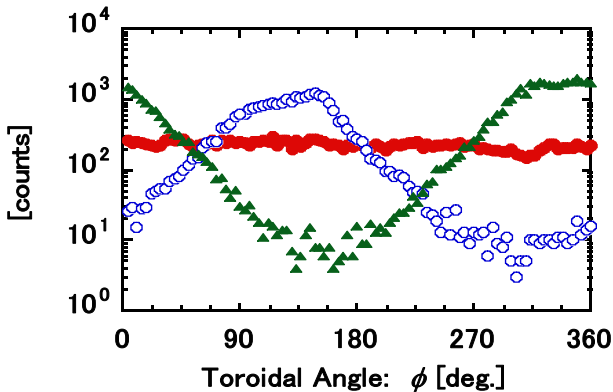


Fig. 4 Variation of neutron detection counts by Fission Chambers (FC) at different locations with the variation of neutron source location during the calibration experiment. The red closed circles, the blue open circles, and green closed triangles indicate the detection count by FCs at NFM#1, the NFM#1, #2, and #3, respectively.

consists from a pair of one  $^{235}\text{U}$  Fission Chamber (FC) and one  $^3\text{He}/^{10}\text{B}$  proportional chamber [11], [21]. An eleven channel Vertical Neutron Camera (VNC) is also installed to investigate the radial profile of neutron at a vertically elongated cross section as shown in Fig.1 [22], [23]. In addition, the Neutron Activation-foil System (NAS) was also installed at two toroidal locations on LHD [24]. The calibration of the NFMs [11] and the NAS [24] were performed circulating a  $^{252}\text{Cf}$  source of 800 MBq in the torus at the midplane. The spatial resolution of the VNC was also examined by an experiment using the source and by the three dimensional general-purpose Monte Carlo N-Particle (MCNP) code calculations [23]. Figure 4 show the result of calibration experiment for FCs at each location of NFM [11]. As shown in Fig.4, the detector counts are almost independent from the toroidal location of the neutrons source at NFM#1, which is installed on the top and at the center of the LHD. On the other hand, significant toroidal angle dependence of detector counts is observed both for NFM#2 and NFM#3, which are installed at the outer side of the LHD torus on the midplane. The detection efficiency of NFMs are evaluated from the toroidal integration of these detection counts, the normalization of the integrated counts and the correction due to the difference of energy spectra between the neutron from the  $^{252}\text{Cf}$  source and the neutron from deuterium plasmas. The detection efficiency is evaluated to be  $1.46 \times 10^8$  neutrons/counts for the FC at NFM#2 [11].

The estimation of neutron emission from LHD plasmas and evaluation of its accuracy are important missions as a commissioning process of the deuterium experiment because the annual neutron yield is limited legally as shown in Table 1 and all of the proposed experiments must be done under this constraint. On LHD, the maximum neutron emission rate of  $1.9 \times 10^{16}$  n/s [1] is expected with the assumption of 35MW heating power, i.e., 18MW with two rNBIs, 14MW with three tNBIs and an additional 3MW with Electron Cyclotron Heating, and with the assumption of the energy confinement time of twice as large as the scaled energy confinement time by the International Stellarator Scaling (ISS) 95 database [25]. The maximum annual neutron yield for the first six years of

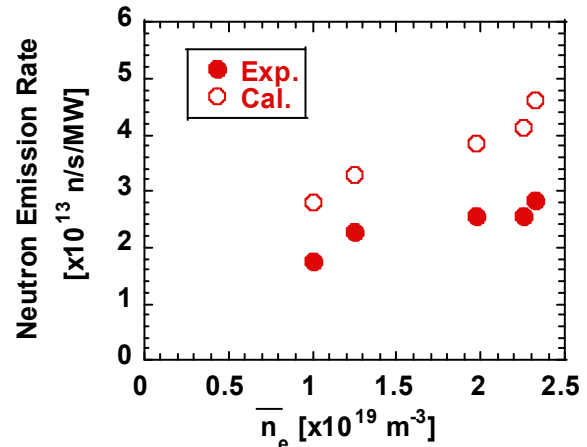


Fig. 5 Line averaged electron density dependence of neutron emission rate from LHD plasmas for deuterium beam injection by NBI#4. The neutron emission rates are normalized by the port-through power of NBI#4. Experiment results are shown by closed circles, while the calculation results of fit3d-dd code are shown by open circles

deuterium experiments correspond to only 368 shots of the expected maximum neutron emission discharge of 3s. Thus, the proper estimation of neutron emission for each proposed experiment is necessary to maximize the use of the LHD deuterium experiments and to minimize the risk in radiation safety. The fit3d-dd code [26], where the neutron emission evaluation function is implemented to fit3d-code [27], [28], is used for this purpose on LHD. In the fit3d-code, the birth points of energetic particles produced by NBIs are calculated by a Monte Carlo routine and their orbit-following calculations were performed after the evaluation of their birth points for a short time interval, i.e., less than their slowing-down times, in order to evaluate the first orbit loss, the orbit averaged minor radii location and the orbit averaged pitch angle. The steady state velocity distribution for the energetic particles is evaluated applying the analytical solution of the Fokker-Planck (FP) equation [29] with the information of the birth points and subsequent orbit following calculations. The neutron emission rate was calculated based on the distribution function and the bulk ion plasma information used in the code.

Figure 5 shows the neutron emission from LHD deuterium plasmas for deuterium beam injection by NBI#4. Neutron emission rates are normalized by the port-through power of NBI#4 in the figure. In evaluating the normalized neutron emission rate by fit3d-dd code, the electron density and temperature profile obtained by the Thomson scattering diagnostic [30] are used. The deuterium ion density is evaluated from the electron density, the fraction of deuterium ion in hydrogen isotopes, and effective charge numbers assuming the charge neutrality of plasma and the shape of ion density profiles are the same as that of electron density profile. The fraction of deuterium ions is evaluated from the intensity ratio of  $H_{\alpha}$  and  $D_{\alpha}$  lines. The fractions are in the range of 0.8 to 0.9 and the effective charge numbers are in the range of 1.5 to 2.5 for the discharges shown in Fig.5. As shown in Fig.5, the estimated neutron emission rate by the fit3d-dd code overestimates the measured neutron emission rate by a factor of two. This seems to be reasonable by considering the fact that only the first orbit loss of energetic deuterium ions is taken into an account and the loss of them during their slowing down process is not considered in the model calculation. For further accurate evaluation of neutron emission rate, the evaluation of energetic deuterium ion velocity distribution by the simulation code which can handle the loss of energetic deuterium ions

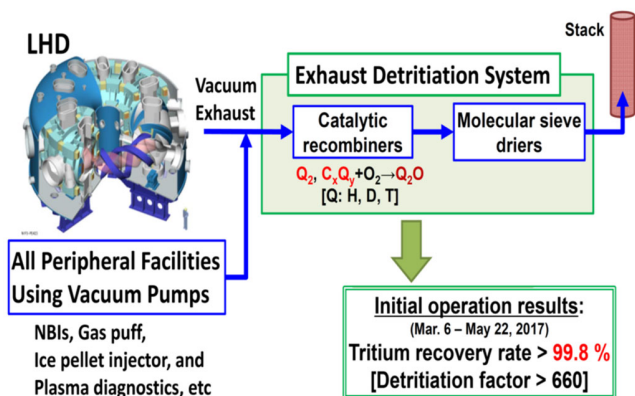


Fig. 6 Schematic Drawing for Exhaust Detritiation System (EDS) on LHD.

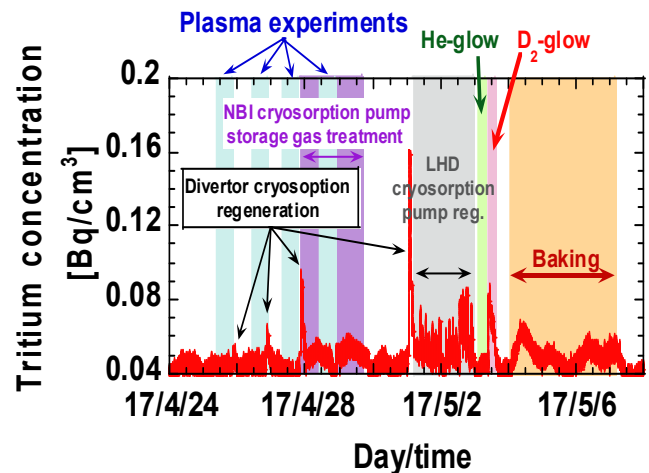


Fig. 7 Variation of tritium concentration measured at the inlet of Exhaust Detritiation System (EDS).

during their slowing down process, e.g., GNET [31], [32], DELTA5D [33] and/or MORH [34] codes, is necessary.

#### IV. EXHAUST DETRITIATION SYSTEM

Based on the agreement for environmental conservation with local government bodies around the NIFS, the Exhaust Detritiation System (EDS), which is often mentioned as Tritium Removal System (TRS), was installed on LHD [1], [5], [35], [36]. To apply the detritiation process entirely to the vacuum exhaust gas from the LHD-VV, all of the vacuum pumps including peripheral devices which share the vacuum of LHD are connected to the EDS as shown in Fig.6. It must be noted that the EDS of the LHD removes all of hydrogen isotopes including tritium from the vacuum exhaust. The EDS consists of two major components. One component is the catalytic recombiner for the oxidation of hydrogen isotope gases and hydrocarbons. The other component is adsorption column which contains molecular sieves. It absorbs all of the water vapors produced by the recombiner. It was confirmed at its initial operation that the recovery rate of hydrogen isotopes, including tritium, exceeded 99.8% in the EDS.

One of the benefits from the installation of the EDS is that the mass balance of hydrogen isotopes in the torus can be evaluated without ambiguity because all of the vacuum exhaust from the LHD-VV was sent to the EDS. In particular, the tritium can be used as a good tracer for monitoring the balance of hydrogen isotopes in LHD because the total amount of tritium produced by the Deuterium experiment can be evaluated from the signals of NFM and because the amount of tritium in the vacuum exhaust is monitored at the inlet of EDS. Figure 7 shows the example of the tritium behavior at the inlet. During the period shown in the figure, the LHD experiments are performed from April 25-28 and light blue regions show the periods when the experiments were performed on these days. The purple region shows the period when the regeneration gas from the NBI cryo-sorption pumps was processed. In processing the regeneration gas from NBI cryo-sorption pumps, a buffer tank was used to store the gas tentatively because the gas exhausting speed from the NBI vacuum pumps exceeds the processing ability of the EDS during the regeneration of

cryo-sorption pumps of the NBIs. Although tritium can be generated in the vacuum vessel of NBI with the reaction between the residual deuterium beam and the deuterium ion which was impinged and stayed in the residual ion dumps, the tritium observed during this period is considered to come from the DD-reaction in LHD-plasmas and to be exhausted through the NBI injection-ports and stored in the cryo-sorption pump in the NBI because the DD reaction that occurred in LHD plasmas is two orders larger than that which occurred in the NBI. The period for the regeneration of the cryo-sorption pumps of LHD-VV pumping system is shown by grey. The tritium exhausted during these periods, i.e., the period of LHD plasma experiments, the regeneration periods of cryo-sorption pumps for LHD-NBI and LHD-VV pumping system, can be considered as a group of tritium directly exhausted from the LHD-VV during the plasma experiment. In Fig.7, the increase of tritium concentration was also observed during the regeneration of the divertor cryo-sorption pump [1], [4]. The increase corresponds to the amount of tritium flowing to the divertor target plates. When a deuterium glow discharge and the baking of LHD-VV are applied, the increase in tritium concentration is also observed. It seems to be reasonable to consider this increase as corresponding to the tritium stored in the plasma counter wall in the LHD-VV because the wall is the most dominant area which directly sees the LHD plasmas. It is interesting that the increase of tritium concentration is not observed during a helium glow discharge. As shown in Fig.7, the monitoring signal of tritium concentration at the inlet of EDS can be used to extract the information of the tritium mass flow in the LHD-VV with proper treatment of LHD-VV and with the proper regeneration of cryo-sorption pumps. This would provide useful information of fuel ion mass flow in the future fusion power plant.

#### V. INITIAL OPERATION OF LHD IN DEUTERIUM

The evaluation of the necessary period to replace hydrogen by deuterium after the start of deuterium experiment (and vice versa) is an important task at the commissioning of the deuterium experiment because the schedule of the future experiment campaign will be determined based on this evaluation to investigate the timing to start the dedicated experiment under full deuterium environment and to investigate the timing to terminate the deuterium experiment in

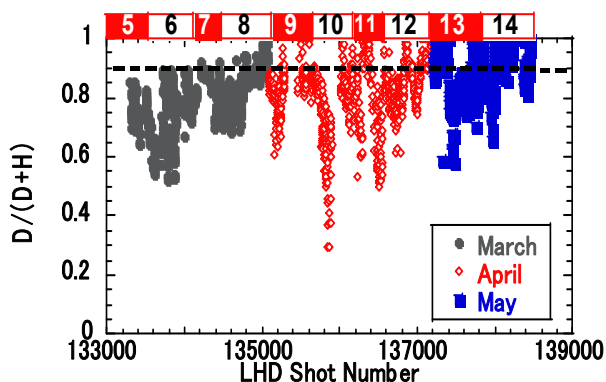


Fig. 8 Change of deuterium fraction in LHD plasmas from the beginning of the deuterium experiment.

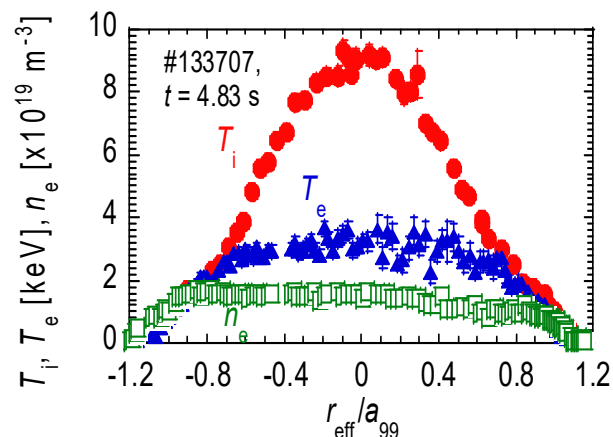


Fig. 9 Ion temperature profile (closed circles), electron temperature profile (closed triangles) and electron density profile (opensquares) of a LHD plasma which exceeds the ion temperature of 9keV.

order to remove the tritium inside the LHD-VV as a preparation for the maintenance period of LHD.

Figure 8 shows the variation of deuterium fraction in hydrogen isotopes in LHD plasmas. The fraction was evaluated from the ratio of  $D_{\alpha}$  and  $H_{\alpha}$  signal intensities. The numbers in bars at the top of the figure indicate the number of weeks from the beginning of the 19<sup>th</sup> LHD experiment cycle. As shown in Fig.8, the fraction of deuterium at the 1st week of the deuterium experiment, i.e., 5th week of the 19th cycle, is about 80% when the deuterium gas puff is performed. The fraction is gradually increased at the subsequent weeks and reached to the saturated level over 90% after four weeks. It seems that four weeks are necessary to replace the hydrogen by deuterium after the introduction of deuterium in LHD. It must be mentioned that the fraction sometimes drops down to 20% by the hydrogen gas puff and/or hydrogen ice pellet injection to investigate the hydrogen ion behavior in deuterium plasmas.

Realization of high performance plasmas, especially high ion temperature plasmas, is the one of the objectives for the deuterium experiment on LHD. On LHD, high ion temperature plasma of 8.1keV was already achieved during the hydrogen operation phase [37], [38], [39]. With the start of the deuterium experiment on LHD, we have successfully realized high ion temperature plasmas exceeding 9keV on LHD. Figure 9 shows an example of ion temperature profile, electron temperature profile, and electron density profile of such a high ion temperature plasma. This realization became possible partly due to the increase of the rNBI injection power in deuterium operation. The isotope effect on the confinement will be evaluated in the future for these high ion temperature discharges applying the TASK3D-a code [40], which is under benchmarking for deuterium discharges. In these discharges, the difference in impurity behavior was observed compared to the similar discharges in the hydrogen experiment. The isotope effect in confinement might appear through the difference in impurity behavior because the impurity has some influence on the confinement property of high ion temperature plasmas on LHD [41].

## VI. CONCLUSION

The deuterium experiment started on March 7th, 2017 on the Large Helical Device (LHD) as a part of LHD's high-performance upgrade project which includes the upgrade of heating devices, the installation of closed helical divertor [1], and the upgrades for diagnostic systems. The objectives of the deuterium experiment is (1) to realize the high performance operation in deuterium, (2) to explore the physics of isotope effect, (3) to demonstrate the confinement capability of energetic particles in helical devices, and (4) to explore the research on PMI using the benefit of the stable steady state operation ability of LHD.

The positive-ion based NBIs were upgraded for deuterium operation increasing their injection energy from 40keV to 60/80keV. Their upgrade is successful and their injection power was increased from 6MW to 9MW. On the other hand, the injection energy of negative-ion based NBIs remains the same. There was concern that their injection power might degrade 70% of the injection power in hydrogen operation when they operate with deuterium due to the mass dependence of optimum beam optics, based on the Child-Langmuir law. It was found that the injection power of the negative-ion based NBI was degraded by almost one-half of the hydrogen operation in order to suppress the heat load onto the electrodes due to the increased fraction of co-extracted electron by the isotope effect in negative-ion sources.

The neutron diagnostic is newly installed for the deuterium experiment and is the most important diagnostic in the experiment. Three sets of NFMs, an eleven channel VNC, and two stations for NAS are installed for the deuterium experiment on LHD. The absolute calibration of NFM and NAS were performed using a <sup>252</sup>Cf neutron source by circulating the source inside the torus at the midplane during the maintenance period of LHD. The neutron yield estimation is important in the deuterium experiment because the annual neutron yield is legally limited. The neutron emission rate is estimated using the fit3d-dd code on LHD. As a task of commissioning, the estimated neutron emission rates are compared to the results of experiment. The neutron emission rate estimated by the code is roughly two times larger than the experiment results. This is due to the model used by the code, where the loss of energetic particles during their slowing down process is not taken into account. The evaluation by the fit3d-dd code is acceptable for the safety radiation control of the deuterium experiment, but more accurate evaluation based on the orbit following Monte-Carlo calculation is desired.

The EDS is also newly installed for the deuterium experiment on LHD. The tritium recovery rate exceeding 99.8% at the EDS was confirmed by its initial operation. To treat all of the exhaust gas from the LHD-VV, all of the outlets of vacuum pumping systems which share the LHD vacuum are connected to the EDS. One of the benefits from the EDS installation is the ability to evaluate the mass balance of fuel ions using the DD produced tritium as a tracer.

The variation of deuterium fraction was examined after the beginning of deuterium experiment. We found that the initial deuterium fraction was about 80% when the deuterium gas puff was performed and it exceeded to 90% within four weeks. The initial deuterium operation of LHD was quite successful. The

ion temperature range of LHD was extended over 9keV with the deuterium operation.

## ACKNOWLEDGMENTS

The first author, M.O., wish to thank the Director General of the National Institutes of Natural Sciences, Prof. Akio Komori, for his continuous encouragement to realize the LHD deuterium experiment. The authors also wish to thank the LHD deuterium experiment preparation group for the enormous effort and great work done in realizing the deuterium experiment. The continuous effort by the LHD-NBI team for optimizing the NBI operation in deuterium is greatly acknowledged. The LHD experiment and all of NIFS activities have been continuously and strongly supported by The Ministry of Education, Culture, Sports, Science and Technology (MEXT), Japan, and domestic and international collaborators. This work was supported by NIFS11ULGG801, NIFS10ULPP701, NIFS11ULPP801, NIFS11ULPP802, NIFS10ULRR701, NIFS10ULRR702, NIFS11ULRR801, NIFS11ULRR802, NIFS11ULRR804, NIFS10ULAA003, NIFS10ULAA701, NIFS10ULAA704, NIFS10ULAA705, NIFS15ULAA708, and 10201042KEIN1601.

## REFERENCES

- [1] M. Osakabe, et al., "Current status of Large Helical Device and its prospect for Deuterium experiment", *Fusion Sci., Tech.*, accepted
- [2] T. Morisaki et al., "Initial Experiments Towards Edge Plasma Control with a Closed Helical Divertor in LHD", *Nucl. Fusion*, **53**(2013) 063014
- [3] S. Masuzaki et al., "Neutral Gas Compression in the Helical Divertor with a Baffle Structure in the LHD Heliotron", *Plasma Fusion Res.*, **6** (2011) 1202007
- [4] T. Murase, et al., "Development of New Concept In-Vessel Cryo-Sorption Pump for LHD Closed Helical Divertor", *Plasma Fusion Res.*, **11** (2016)1205030
- [5] Y. Takeiri, et al., "Prospect towards steady-state helical fusion reactor based on progress of LHD project entering the deuterium experiment phase", The 27<sup>th</sup> IEEE SOFE, 2017 (submitted to IEEE)
- [6] M. Bessenrodt-Weberpals et al., "The Isotope Effect in ASDEX", *Nucl. Fusion*, **33** (1993) 1205
- [7] S. D. Scott et al. "Isotopic Scaling of Confinement in Deuterium-Tritium Plasmas", *Phys. Plasmas*, **2** (1995) 2299
- [8] R. J. Hawryluk et al., "Results from Deuterium-Tritium Tokamak Confinement Experiments", *Rev. Mod. Phys.*, **70** (1998) 537
- [9] J. Jacquinet et al., "Deuterium-Tritium Operation in Magnetic Confinement Experiments: Results and Underlying Physics", *Plasma Phys. Control. Fusion*, **41** (1999) A13
- [10] H. Urano et al., "Energy Confinement of Hydrogen and Deuterium H-mode Plasmas in JT-60U", *Nucl. Fusion*, **52** (2012) 114021
- [11] M. Isobe, et al, "Neutron Diagnostics in the Large Helical Device", The 27<sup>th</sup> IEEE SOFE, 2017 (submitted to IEEE)
- [12] Y. Takeiri, et al., "High Performance of Neutral Beam Injectors for Extension of LHD Operational Regime", *Fusion Sci. Tech.*, **58** (2010) 482
- [13] K. Tsumori, et al., "Research and Development Activities on Negative Ion Sources", *Fusion Sci. Tech.*, **58** (2010) 489
- [14] T. Inoue, et al., "Comparison of H<sup>+</sup> and D<sup>+</sup> Production in a Magnetically Filtered Multicusp Source", *Rev. Sci. Instrum.* **61** (1990) 496
- [15] C. Wimmer, et al., "Extraction of Negative Charges from an Ion Source: Transition from an Electron repelling to an Electron attracting Plasma Close to the Extraction Surface", *J. Appl. Phys.*, **120** (2016) 073301
- [16] J. R. Coupland, et al., "A study of the Ion Beam Intensity and Divergence Obtained from a Single Aperture Three Electrode Extraction System", *Rev. Sci. Instrum.* **44** (1973) 1258

- [17] O. Kaneko, et al., "Plasma Startup by Neutral Beam Injection in the Large Helical Device", Nucl. Fusion, **39** (1999) 1087
- [18] O. Kaneko, et al., "Analysis of Plasma Initiation by Neutral Beam in the Large Helical Device", Nucl. Fusion, **42** (2002) 441
- [19] O. Kaneko, et al., "Plasma Initiation by Neutral Beam Injection", Fusion Sci. Tech., **58** (2010) 497
- [20] R. Ito, et al., "Analytic Cross Sections for Collisions of H, H<sub>2</sub>, He and Li Atoms and Molecules I", JAERI-M 93-1
- [21] M. Isobe et al., "Wide Dynamic Range Neutron Flux Monitor Having Fast Time Response for the Large Helical Device", Rev. Sci. Instrum., **85** (2014) 11E114
- [22] K. Ogawa et al., "Progress in Development of the Neutron Profile Monitor for the Large Helical Device", Rev. Sci. Instrum., **85** (2014) 11E110
- [23] H. Kawase, et al., "Evaluation of spatial resolution of neutron profile monitor in LHD", This conference (submitted to IEEE)
- [24] N. Pu, et al., "In situ Calibration of Neutron Activation System on the Large Helical Device", submitted to Rev. Sci. Instrum.,
- [25] U. Stroth et al., "Energy Confinement Scaling from the International Stellarator Database", Nucl. Fusion, **36** (1996) 1063
- [26] M. Homma, et al., "Simulation Study of Energetic Triton Confinement in the D-D Experiment on LHD", Plasma and Fusion Research **10** (2015) 3403050
- [27] S. Murakami, et al., "Finite  $\beta$  Effects on the ICRF and NBI Heating in the Large Helical Device", Trans. Fusion Technol., **27** (1995) .256
- [28] P. Vincenzi, et al., "Upgrades and application of FIT3D NBI plasma interaction code in view of LHD deuterium campaigns", Plasma Phys. Control. Fusion, **58** (2016) 125008
- [29] J. A. Rome, et al., "Particle-orbit Loss Regions and their Effects on Neutral-Injection Heating in Axisymmetric TOKAMAKs", Nucl. Fusion, **16** (1976) 55
- [30] I. Yamada, et al., "Recent Progress of the LHD Thomson Scattering System", Fusion Sci Tech., **58** (2010) 345
- [31] S. Murakami, et al., "Effect of Neoclassical Transport Optimization on Energetic Ion Confinement in LHD", Fusion Sci Tech., **46** (2010) 241
- [32] S. Murakami, et al., "A global simulation study of ICRF heating in the LHD", Nucl. Fusion **46** (2006) S425
- [33] D. A. Spong, et al., "Confinement Properties of Small Aspect Ratio Tokamak/Stellarator Hybrid Devices", Plasma Phys. Rep., **23** (1997) 523
- [34] R. Seki, et al., "Monte Carlo Study Based on a Real Coordinate System for Tangentially Injected High-Energy Particles in the Large Helical Device", Plasma Fusion Res., **5** (2010) 27
- [35] M. Tanaka, et al., "Observations of the gas stream from the Large Helical Device for the design of an exhaust detritiation system", Plasma Fusion Res., **11** (2016) 2405055
- [36] M. Tanaka, et al., "Design and commissioning of the exhaust detritiation system for the Large Helical Device", submitted to Fusion Eng. Des.,
- [37] K. Nagaoka, et al., "Integrated Discharge Scenario for High-Temperature Helical Plasma in LHD", Nucl. Fusion, **55** (2015) 113020
- [38] H. Takahashi, et al., "Extension of Operational Regime in high-temperature plasmas and Effect of ECRH on ion thermal transport in the LHD", Nucl. Fusion **57** (2017) 086029
- [39] Y. Takeiri, et al., "Extension of operational regime of LHD towards deuterium experiment", Nuclear Fusion accepted
- [40] M. Yokoyama, et al., "Extended capability of the integrated transport analysis suite, TASK3D-a, for LHD experiment", Nucl. Fusion accepted
- [41] M. Osakabe, et al., "Impact of carbon impurities on the confinement of high-ion-temperature discharges in the Large Helical Device", Plasma Phys. Control. Fusion, **56** (2014) 095011